Development and validation of a finite-element musculoskeletal model incorporating a deformable contact model of the hip joint during gait

Junyan Li

Institute:

School of Science and Technology, Middlesex University, London, UK

Key words: Musculoskeletal modelling; finite element; contact mechanics; articular cartilage; hip joint; gait

Corresponding author:

Junyan Li

ljyjerry@gmail.com

School of Science and Technology, Middlesex University, London, United Kingdom NW4 4BT

Abstract

Musculoskeletal models provide non-invasive and subject-specific biomechanical investigations of the musculoskeletal system. In a musculoskeletal model, muscle forces contribute to the deformation and kinematics of the joint which in turn would alter moment arms of muscles and ground reaction forces and thus affect the prediction of muscle forces and contact forces and contact mechanics of the joint. By far, deformable contact models of the hip have not been considered in musculoskeletal models, and the role of kinematics and deformation within the hip in muscle forces and hip contact mechanics is unknown. In this study, an FE musculoskeletal model including bones, joints and muscles of the lower extremity was developed. A deformable contact model of the hip joint was incorporated and coupled into the musculoskeletal model. Joint angles and ground reaction forces during gait were used as inputs. Optimization minimizing the sum of muscle stresses squared was performed directly to the FE musculoskeletal model in order to simultaneously solve muscle forces and contact forces and contact stresses of the hip joint within a single framework. The calculated hip contact forces corresponded well to the *in vivo* measurement data. The maximum hip contact stress was 6.5 MPa and occurred at weight-acceptance. The influence of kinematics and deformation in the hip on muscles forces and hip contact forces was minimal and not sensitive to variations in the thickness and properties of the joint cartilage during gait. This suggests that the uncoupled approach in which the hip contact forces and contact mechanics are simulated in separate frameworks would serve as an effective and efficient alternative for subject-specific modelling of the hip. This study provides guidance for the level of complexity needed for future hip models and can be used to evaluate biomechanical changes of the musculoskeletal system following interventions.

1. Introduction

Numerical analyses allow for non-invasive and systematic biomechanical evaluation of the hip joint. For example, finite-element (FE) models have been widely used to study stresses and strains within the hip (Henak et al., 2014, Li et al., 2016). These regional hip models require contact forces of the joint as inputs. Therefore, musculoskeletal models of the lower extremity bridging the body kinematics and joint biomechanics are needed for non-invasive and subject-specific studies.

Previous musculoskeletal models (e.g. OpenSim (Delp et al., 2007) and AnyBody (AnyBody Technology, Denmark)) have been mostly constructed in multi-body dynamics with the model assumed as rigid and the hip as a simple three degrees-of-freedom (DOFs) rotational joint (Li et al., 2015). Based on kinematics and kinetics of the lower extremity, these multi-body dynamics models have been primarily used to determine contact forces of the joint which then serve as inputs for FE models of the joint region to simulate its contact mechanics (i.e. uncoupled simulation) (Farrokhi et al., 2011). Contact joint models have been recently incorporated into multi-body dynamics musculoskeletal models by calculating contact forces between rigid bodies based on their overlapping volume (Zhang et al., 2015). However, in this approach, the joint kinematics contributed by the cartilage deformation cannot be realistically simulated.

In a musculoskeletal model, muscle forces contribute to the deformation and kinematics of the joint which in turn would alter moment arms of muscles and ground reaction forces and thus affect the prediction of muscle forces and contact forces and contact mechanics of the joint. This interaction was found to have a marked effect on the biomechanics of the knee through some recent attempts in which the knee joint was presented in detail and coupled into a musculoskeletal model (Marouane et al., 2017, Shu et al., 2018, Hume et al., 2019), but remains unknown for the hip. In order to consider the interaction between muscle forces and kinematics and contact mechanics in the joint, incorporation of deformable and contact joint models into musculoskeletal models is needed. However, such models involve more complex construction and optimization procedures and longer simulation periods (Shu et al., 2018, Hume et al., 2019), compared with the uncoupled approach simulated in separate frameworks. So far, deformable contact models of the hip have not been considered in musculoskeletal models, and the role of kinematics and deformation within the hip in muscle forces and hip contact mechanics is poorly understood. This information provides important guidance for the level of complexity needed for future musculoskeletal models focused on the hip joint, so that a reasonable balance between accuracy and efficiency for numerical simulations of the hip joint can be determined.

The aim of this study was to develop and validate an FE musculoskeletal model of the lower extremity incorporating a deformable contact model of the hip joint. Additionally, the effect of kinematics within the hip on muscle forces and hip contact mechanics was evaluated by comparing the predictions of this coupled model to an uncoupled model in which contact forces and contact stresses of the hip were simulated using separate frameworks.

2. Methods

2.1. Musculoskeletal model

The FE musculoskeletal model was developed in an implicit FE solver FEBio (version 2.6.4; http://febio.org/febio). The model included the bones and joints of the right lower extremity and the complete set of muscles driving the hip which were modelled as contractile forces (**Fig. 1a**) (Carbone et al., 2015). The insertion and origin of the muscles were revised based on the refined TLEM 2.0 model (De Pieri et al., 2018). To ensure proper computational efficiency, the muscles that do not cross the hip joint were excluded; the knee and ankle were assumed as simple three DOFs rotational joints and bones as rigid, with the patella immobilized onto the tibia (Li et al., 2015).

A natural hip model from a 55 year-old, 109 kg, 180 cm male was incorporated into the FE musculoskeletal model, considering the cartilage with subject-specific geometry (Li et al., 2016). The modelling of the hip joint is based on a previously validated procedure (Li et al., 2014). The back surfaces of the cartilage were bonded onto the underlying bones. Frictionless contact between the cartilage layers was defined, with the surface of the femoral head cartilage as the master and the surface of the acetabular cartilage as the slave. The cartilage and bones were represented by 11460 eight-noded hexahedral elements and 6145 four-noded tetrahedral elements, respectively. The mesh density of the cartilage was evaluated to ensure that the differences in the peak contact stress were below 5% when the number of elements was doubled. Neo-Hookean material was adopted as the baseline constitutive model of the cartilage, with strain energy given by:

$$W = \frac{1}{2}\mu(\tilde{I}_1 - 3) + \frac{1}{2}K(\ln(J))^2 \tag{1}$$

Where, $\tilde{I}_1$ is the first deviatoric invariant of the right Cauchy deformation tensor; J Jacobian of the deformation; μ shear modulus; K bulk modulus. The cartilage material was reinforced by fibres with isotropic distribution. The fibre strain energy is given by:

$$W_f = \int_A H\,(\tilde{I}_n - 1)\,\xi(\mathbf{n})\,(\tilde{I}_n - 1)^{\beta(\mathbf{n})} dA \tag{2}$$

Where, $\tilde{I}_n$ is the square of the deviatoric fibre stretch; **n** the unit vector along the fibre direction; The integral is evaluated over the unit sphere A spanned by all directions **n**; $H(\text{-})$ the unit step function ensuring that fibres only sustain tension; ξ scales the fibre response; β controls the nonlinearity of fibres. Refer to (Maas and Weiss, 2007) for further description of the constitutive model. Coefficients of the constitutive model were defined as: μ = 1.82 MPa, K = 1860 MPa, ξ = 9.19 MPa, and β = 4 (Henak et al., 2014).

2.2. Subject and gait data

Inputs of the FE musculoskeletal model including joint angles and ground reaction forces are based on the gait data of a patient (named as H2R in the database; a 62 year-old, 78 kg, 172 cm male) with an instrumented hip implant during walking (https://orthoload.com/) (Bergmann et al., 2016). The FE musculoskeletal model was linearly scaled to match the anthropometry of the patient's lower extremity. As the simulation was quasi-static and the inertia effect not considered, the pelvis was immobilized along the three translational DOFs. The rotational angles of the pelvis (relative to the global coordinate system), hip, knee and ankle of the patient were derived from the marker trajectories in the gait data using Visual 3D (V6; C-Motion, USA). These angles were then used to rotate the pelvis, hip, knee and ankle in the musculoskeletal model. The ground reaction forces and moments along the axes of the global coordinate system were distributed onto the heel and toe of the musculoskeletal model according to the locomotion of the ground reaction forces on the force plates, so that these forces and moments were applied onto the proper position of the foot.

2.3. Calculation of muscle forces and hip contact mechanics

An optimization approach was developed in this study to solve the muscle redundancy issue in the musculoskeletal system (i.e. muscles outnumber the equations of equilibrium, requiring optimization to determine a unique solution of muscle forces). Based on the muscle forces and the corresponding joint moments in the FE musculoskeletal model, the muscle forces were optimized until the sum of the square of muscle stresses (i.e. muscle force over physiological cross-sectional area) was minimized, and at the same time, the resultant hip moment approached zero. The “fmincon” optimization tool in MATLAB (R2017a, Mathworks, MA) was adopted to solve the optimization problem. Both the FE simulation and the optimization were continuous, e.g. simulation of the FE musculoskeletal model at 0.5s starting from the optimized model at its previous time instance (i.e. 0.45s). The outputs of the model including muscle forces and contact forces, contact stresses and kinematics of the hip were analysed at 14 evenly distributed time instances of the stance phase of a gait, starting from heel-strike (0s, 0%) to toe-off (0.65s, 100%). Kinematics of the hip was calculated as the translational displacement of the femoral head center relative to the acetabulum center.

In order to validate the model, the hip contact forces predicted by the FE musculoskeletal model were compared to the *in vivo* measurement data during the same gait trial. Additionally, a musculoskeletal model with three DOFs rotational hip joint was developed and its predicted contact forces and kinematics of the hip were then used as the inputs of a regional FE model of the same hip joint (**Fig. 1b**). Results of this uncouple simulation (i.e. uncoupled model) were compared to the original musculoskeletal model incorporating a contact hip joint (i.e. coupled model), in order to evaluate the effect of kinematics and deformation of the hip joint on its contact mechanics and muscle forces.

In this study, only one subject was investigated. However, different subjects have various geometry and properties of the hip cartilage, which might lead to altered conclusion regarding the influence of hip kinematics and deformation on hip contact mechanics and muscle forces. To account for the variations in the thickness and properties of the joint cartilage, a sensitivity study was conducted by performing the comparison (i.e. coupled approach VS uncoupled approach) using four other models that were constructed based on the original cartilage model: Model 2 with approximately 25% thicker cartilage (Shepherd and Seedhom, 1999); Model 3 with approximately 25% thinner cartilage; Model 4 with 50% higher μ and ξ; Model 5 with 50% lower μ and ξ

(Athanasiou et al., 1994). Models 3 and 4 were developed by removing/adding a layer of elements based on the original model.

Results

As shown in **Fig. 2**, predictions of the FE musculoskeletal model, including the direction and magnitude of the hip contact forces and the timing at heel-strike, weight-acceptance, mid-stance, push-off and toe-off, were in good agreement with the *in vivo* measurement data. Compared to the *in vivo* measurement data, the simulated total hip contact force (i.e. sum of the three vector components in **Fig. 2**) was 25% higher at weight-acceptance, 7% lower at mid-stance and 2% higher at push-off, with a mean absolute percentage error of 15% over the stance cycle.

The difference in the hip contact forces between the coupled (original) and uncoupled models was less than 1% (**Fig. 2**). The magnitude and distribution of the hip contact stresses between the coupled (original) and uncoupled models were also nearly identical (**Fig. 3**). Contact stresses at weight-acceptance and push-off were markedly higher than the other gait phases, with the maximum value of 6.5 MPa that occurred at weight-acceptance (**Fig. 3**). The difference in the forces of the major hip muscles between the coupled (original) and uncoupled models was within 5% (**Fig. 4**). As predicted by the coupled (original) model, kinematics and deformation in the hip occurred during walking was less than 1 mm which was minimal compared to the scale of the joint (**Fig. 5**). In the sensitivity study (Models 2-5), the differences in hip contact forces and muscles forces between the coupled and uncoupled approaches were within 5%.

Discussion

In this study, an FE musculoskeletal model of the lower extremity incorporating a contact model of the hip joint was developed for the first time. Optimization was performed directly to the FE musculoskeletal model in order to simultaneously solve the muscle forces and the contact forces and contact stresses of the hip joint within a single framework. The hip contact forces predicted by the model corresponded well to the *in vivo* measurement data over the entire stance cycle. The maximum contact stress in the hip during walking predicted by the model was 6.5 MPa under a load of 1982 N which is consistent with previous *in vitro* measurements (4–10 MPa under loads of 2500 N–3000 N) (Brown and Shaw, 1983, Afoke et al., 1987, Anderson et al., 2008).

FE musculoskeletal models incorporating deformable contact joints enable simulations of the interaction between muscle forces and joint kinematics/deformation which cannot be accounted for in the widely used multi-body dynamics musculoskeletal models, allowing for more systematic and realistic biomechanical analyses of the musculoskeletal system, but at the same time involving more complex and lengthy simulations

(Shu et al., 2018, Hume et al., 2019, Sharifi et al., 2020). Using 8 CPU cores, the simulations of the coupled model and uncoupled model required 3 days and 3.5 hours, respectively. In this study, it was found that kinematics and deformation in the natural hip joint was markedly smaller than the dimension of the hip and the moment arms of muscles and ground reaction forces, and thus had a minimal effect on the muscles forces and hip contact forces calculated through musculoskeletal models. This suggests that the uncoupled approach in which the loading and contact mechanics of the hip are simulated in separate frameworks would serve as an effective and efficient alternative for subject-specific modelling of the hip. This finding is further supported by the sensitivity study in which it was found that variations in the geometry and material properties of the hip cartilage had a minimal effect on the hip contact forces and muscle forces. As a healthy hip joint during walking was evaluated in this study, further analyses should be performed for other activities and for hips in dysplasia in which the joint is less congruent than a healthy hip and its kinematics might have an evident influence on the muscle forces and hip contact mechanics (Lequesne et al., 2004).

There are some limitations. First, the optimization was performed only for the hip joint. Including multiple joints in the optimization requires extra muscles and increased computational expenses, but would enable more realistic modelling. As found by Adouni and Shirazi-Adl (2013), inclusion of the hip joint in the optimization of the knee and ankle joints slightly influences the calculation of muscle forces and contact forces of the knee. Furthermore, consideration of the muscles across the other joints (e.g. knee) would also improve the modelling accuracy, as these muscles might affect the calculation of hip muscle forces and the resultant joint contact forces. Another limitation is that parameters of the muscle including its passive properties, 3D geometry, large attachment areas, spatial fibre alignment within muscles, and contact and wrapping between muscles and surrounding tissues are important for the accuracy of musculoskeletal modelling but were not considered in this study. These aspects can be accounted for by incorporating 3D muscles into musculoskeletal models which require a lengthy period of simulations (Li et al., 2019). Additionally, ligaments and capsules were not accounted for, because these soft tissues were found to contribute slightly to the kinematics and contact mechanics of the hip in a musculoskeletal model representing these tissues as a 1D spring (Zhang et al., 2015). However, the role of ligaments and capsules in the hip should be further assessed using detailed 3D models. Future development will focus on creating a hybrid musculoskeletal model incorporating both 1D and 3D muscles and other soft tissues as a reasonable compromise between accuracy and efficiency. The labrum was excluded because it provides little assistance in load bearing of the hip (Henak et al., 2011). The time-dependent biphasic/viscoelastic properties of the cartilage was not considered, because it is highly time-consuming to achieve numerical convergence in biphasic simulations and the time-dependent response of the hip cartilage is minimal during short term loading (Li et al., 2013, Li et al., 2016, Todd et al., 2018).

Generally, the hip contact forces predicted by the computer model corresponded reasonably well to the *in vivo* measurement over the entire stance cycle. The difference in comparison might be due to several reasons, apart from the model simplification described in the paragraph above and errors of the *in vivo* measurement. First, the boundary conditions of the experimental models were derived from the gait data of a patient with an instrumented hip implant for the purpose of validation, whereas the musculoskeletal model and geometric model of the finite element hip joint were from subjects with healthy hip joints. Validation and *in vivo* measurement of biomechanics in healthy hip joints are challenging, but should be attempted, e.g., through imaging measurements and validation of soft tissue deformation and joint kinematics using the same subject. Secondly, muscle forces predicted by the models were not compared to the experimental data such as electromyography (EMG) signals, because of uncertainties in acquisition and conversion of EMG signals. Although validation of muscle forces was not within the scope of the current study, inclusion of experimentally measured muscle activity either in the validation or among the model inputs would contribute to the accuracy and validity of future models focusing on biomechanics of muscles.

In this study, a musculoskeletal model with a contact joint was developed within a single finite element framework, with optimization integrated into the finite element simulation process. This enables simulations of 3D geometries, deformation and biotribology of joints, bones, muscles (Li et al., 2019) and other tissues within musculoskeletal models. The modelling framework also allows for multi-scale analyses, considering interactions between models at different scales spanning from the skeletal scale to the tissue and micro scales. Additionally, the modelling framework can be used to evaluate biomechanical changes of the musculoskeletal system following interventions.

Acknowledgements

Efforts of the TLEM 2.0, FEBio and OrthoLoad developers are appreciated. This research benefits from the Newton Fund 2017-RLWK9-10075.

Conflict of interest

The author declares no conflict of personal or financial interests.

References

ADOUNI, M. & SHIRAZI-ADL, A. 2013. Consideration of equilibrium equations at the hip joint alongside those at the knee and ankle joints has mixed effects on knee joint response during gait. *Journal of Biomechanics,* 46, 619-624.

AFOKE, N. Y., BYERS, P. D. & HUTTON, W. C. 1987. Contact pressures in the human hip joint. *Journal of Bone and Joint Surgery (British),* 69, 536-41.

ANDERSON, A. E., ELLIS, B. J., MAAS, S. A., PETERS, C. L. & WEISS, J. A. 2008. Validation of finite element predictions of cartilage contact pressure in the human hip joint. *Journal of Biomechanical Engineering,* 130, 051008.

ATHANASIOU, K. A., AGARWAL, A. & DZIDA, F. J. 1994. Comparative study of the intrinsic mechanical properties of the human acetabular and femoral head cartilage. *Journal of Orthopaedic Research,* 12, 340-349.

BERGMANN, G., BENDER, A., DYMKE, J., DUDA, G. & DAMM, P. 2016. Standardized loads acting in hip implants. *PLOS ONE,* 11, e0155612.

BROWN, T. D. & SHAW, D. T. 1983. In vitro contact stress distributions in the natural human hip. *Journal of Biomechanics,* 16, 373-384.

CARBONE, V., FLUIT, R., PELLIKAAN, P., VAN DER KROGT, M. M., JANSSEN, D., DAMSGAARD, M., VIGNERON, L., FEILKAS, T., KOOPMAN, H. F. J. M. & VERDONSCHOT, N. 2015. TLEM 2.0 – A comprehensive musculoskeletal geometry dataset for subject-specific modeling of lower extremity. *Journal of Biomechanics,* 48, 734-741.

DE PIERI, E., LUND, M. E., GOPALAKRISHNAN, A., RASMUSSEN, K. P., LUNN, D. E. & FERGUSON, S. J. 2018. Refining muscle geometry and wrapping in the TLEM 2 model for improved hip contact force prediction. *PLOS ONE,* 13, e0204109.

DELP, S. L., ANDERSON, F. C., ARNOLD, A. S., LOAN, P., HABIB, A., JOHN, C. T., GUENDELMAN, E. & THELEN, D. G. 2007. OpenSim: Open-Source Software to Create and Analyze Dynamic Simulations of Movement. *Biomedical Engineering, IEEE Transactions on,* 54, 1940-1950.

FARROKHI, S., KEYAK, J. H. & POWERS, C. M. 2011. Individuals with patellofemoral pain exhibit greater patellofemoral joint stress: a finite element analysis study. *Osteoarthritis and Cartilage,* 19, 287-294.

HENAK, C. R., ATESHIAN, G. A. & WEISS, J. A. 2014. Finite element prediction of transchondral stress and strain in the human hip. *Journal of Biomechanical Engineering,* 136, 021021-021021.

HENAK, C. R., ELLIS, B. J., HARRIS, M. D., ANDERSON, A. E., PETERS, C. L. & WEISS, J. A. 2011. Role of the acetabular labrum in load support across the hip joint. *Journal of Biomechanics,* 44, 2201-2206.

HUME, D. R., NAVACCHIA, A., RULLKOETTER, P. J. & SHELBURNE, K. B. 2019. A lower extremity model for muscle-driven simulation of activity using explicit finite element modeling. *Journal of Biomechanics,* 84, 153-160.

LEQUESNE, M., MALGHEM, J. & DION, E. 2004. The normal hip joint space: variations in width, shape, and architecture on 223 pelvic radiographs. *Annals of the Rheumatic Diseases,* 63, 1145.

LI, J., HUA, X., JONES, A. C., WILLIAMS, S., JIN, Z., FISHER, J. & WILCOX, R. K. 2016. The influence of the representation of collagen fibre organisation on the cartilage contact mechanics of the hip joint. *Journal of Biomechanics,* 49, 1679-1685.

LI, J., LU, Y., MILLER, S., JIN, Z. & HUA, X. 2019. Development of a finite element musculoskeletal model with the ability to predict contractions of three-dimensional muscles. *Journal of Biomechanics,* 94, 230-234.

LI, J., MCWILLIAMS, A. B., JIN, Z., FISHER, J., STONE, M. H., REDMOND, A. C. & STEWART, T. D. 2015. Unilateral total hip replacement patients with symptomatic leg length inequality have abnormal hip biomechanics during walking. *Clinical Biomechanics* 30, 513-519.

LI, J., STEWART, T. D., JIN, Z., WILCOX, R. K. & FISHER, J. 2013. The influence of size, clearance, cartilage properties, thickness and hemiarthroplasty on the contact mechanics of the hip joint with biphasic layers. *Journal of Biomechanics,* 46, 1641-1647.

LI, J., WANG, Q., JIN, Z., WILLIAMS, S., FISHER, J. & WILCOX, R. K. 2014. Experimental validation of a new biphasic model of the contact mechanics of the porcine hip. *Proceedings of the Institution of Mechanical Engineers, Part H: Journal of Engineering in Medicine,* 228, 547-555.

MAAS, S. A. & WEISS, J. A. 2007. *FEBio Theory Manual*, http://mrl.sci.utah.edu/software/febio.

MAROUANE, H., SHIRAZI-ADL, A. & ADOUNI, M. 2017. 3D active-passive response of human knee joint in gait is markedly altered when simulated as a planar 2D joint. *Biomechanics and Modeling in Mechanobiology,* 16**,** 693-703.

SHARIFI, M., SHIRAZI-ADL, A. & MAROUANE, H. 2020. Sensitivity of the knee joint response, muscle forces and stability to variations in gait kinematics-kinetics. *Journal of Biomechanics,* 99**,** 109472.

SHEPHERD, D. E. & SEEDHOM, B. B. 1999. Thickness of human articular cartilage in joints of the lower limb. *Annals of the Rheumatic Diseases,* 58**,** 27-34.

SHU, L., YAMAMOTO, K., YAO, J., SARASWAT, P., LIU, Y., MITSUISHI, M. & SUGITA, N. 2018. A subject-specific finite element musculoskeletal framework for mechanics analysis of a total knee replacement. *Journal of Biomechanics,* 77**,** 146-154.

TODD, J. N., MAAK, T. G., ATESHIAN, G. A., MAAS, S. A. & WEISS, J. A. 2018. Hip chondrolabral mechanics during activities of daily living: Role of the labrum and interstitial fluid pressurization. *Journal of Biomechanics,* 69**,** 113-120.

ZHANG, X., CHEN, Z., WANG, L., YANG, W., LI, D. & JIN, Z. 2015. Prediction of hip joint load and translation using musculoskeletal modelling with force-dependent kinematics and experimental validation. *Proceedings of the Institution of Mechanical Engineers, Part H: Journal of Engineering in Medicine,* 229**,** 477-490.

Figure Legends

Fig. 1. a – coupled model in which a contact model of the natural hip joint was incorporated into an FE musculoskeletal model of the lower extremity (cartilage displayed in yellow). b – uncoupled model in which the hip contact forces calculated in a musculoskeletal model with three DOFs rotational hip joint were used as the inputs for an FE model of the hip region. The musculoskeletal models include 33 unique hip muscles comprised of 97 musculotendon fibres (displayed in red).

Fig. 2. Contact forces in the hip predicted by the musculoskeletal models in comparison with the *in vivo* measurement data (Bergmann et al., 2016). Force components along the anterior-posterior (AP), superior-inferior (SI) and lateral-medial (LM) directions in the lab/global coordinate system are illustrated. The simulated hip contact forces corresponded well to the *in vivo* measurement data. The hip contact forces between the coupled (original) and uncoupled models were nearly identical. In the sensitivity study, hip contact forces of the models with varying thickness and material properties of the cartilage (Models 2-5) were approximately overlapped with the current plots (original model).

Fig. 3. Contour of contact stress on the surface of acetabular cartilage at characteristic gait phases predicted by the coupled (original) model, in comparison to the uncoupled model. The magnitude and distribution of the hip contact stresses between these two models were nearly identical. Contact stresses at weight-acceptance and push-off were markedly higher than the other gait phases, with the maximum value of 6.5 MPa that occurred at weight-acceptance.

Fig. 4. Forces of the major hip muscles predicted by the coupled (original) model, in comparison to the uncoupled model. The difference in the muscles forces between these two models was less than 5%. In the sensitivity study, muscle forces of the models with varying thickness and material properties of the cartilage (Models 2-5) were approximately overlapped with the current plots (original model).

Fig. 5. Kinematics of the hip in the coupled (original) model, calculated as the translational displacement of the femoral head center relative to the acetabulum center. Kinematics of the hip occurred during walking was less than 1 mm and was minimal compared to the scale of the hip joint. When the peak kinematics of the hip occurred, the peak value of the maximum compression strain was 0.12 (shown in cross-sectional view).

Fig. 1

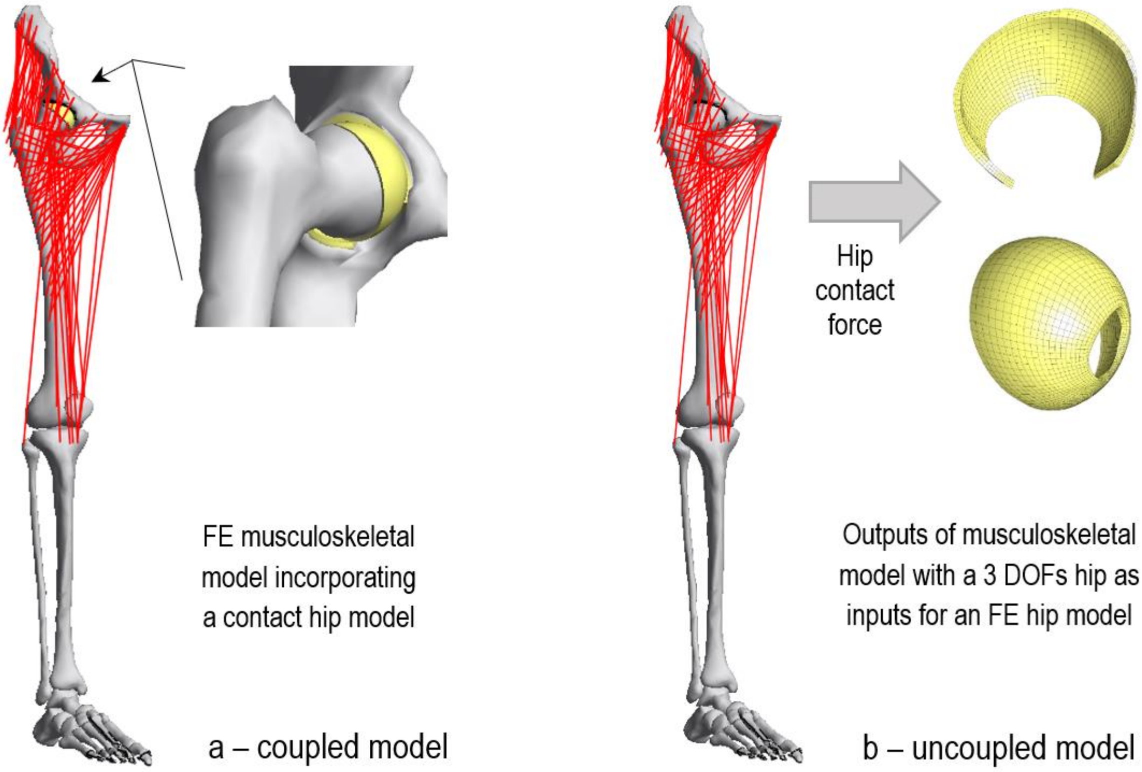
Hip
contact
force
FE musculoskeletal
model incorporating
a contact hip model
a – coupled model
Outputs of musculoskeletal
model with a 3 DOFs hip as
inputs for an FE hip model
b – uncoupled model

Fig. 2

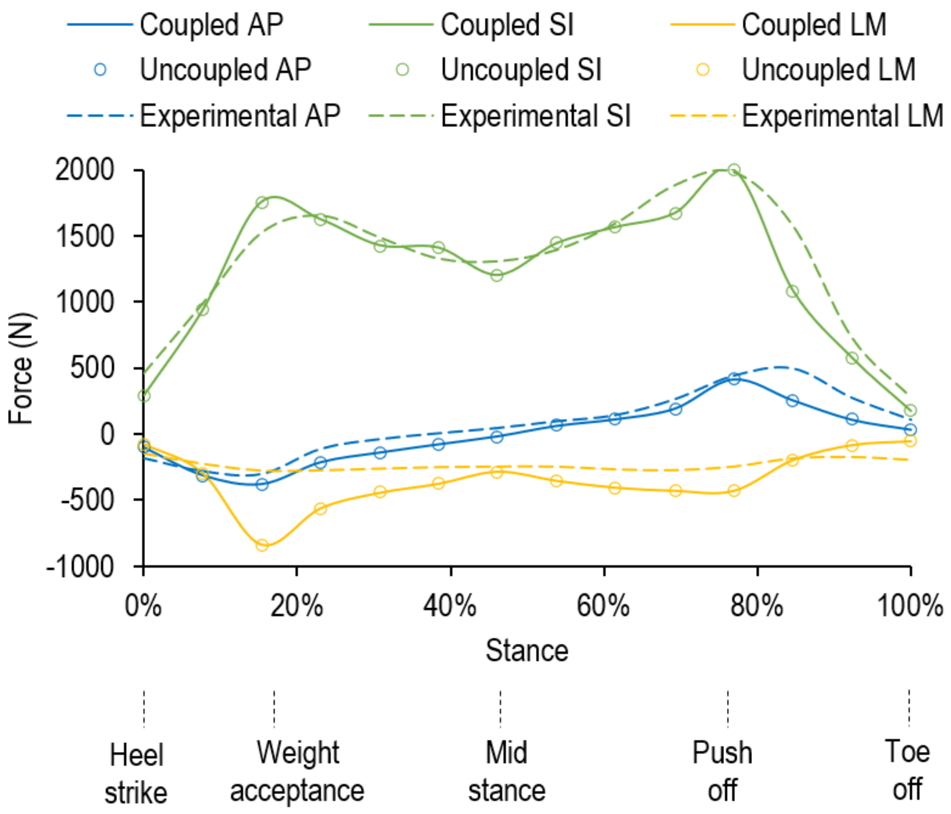

Coupled AP
Coupled SI
Coupled LM
Uncoupled AP
Uncoupled SI
Uncoupled LM
Experimental AP
Experimental SI
Experimental LM
2000
1500
1000
500
0
-500
-1000
Force (N)
0%
20%
40%
60%
80%
100%
Stance
Heel strike
Weight acceptance
Mid stance
Push off
Toe off

Fig. 3

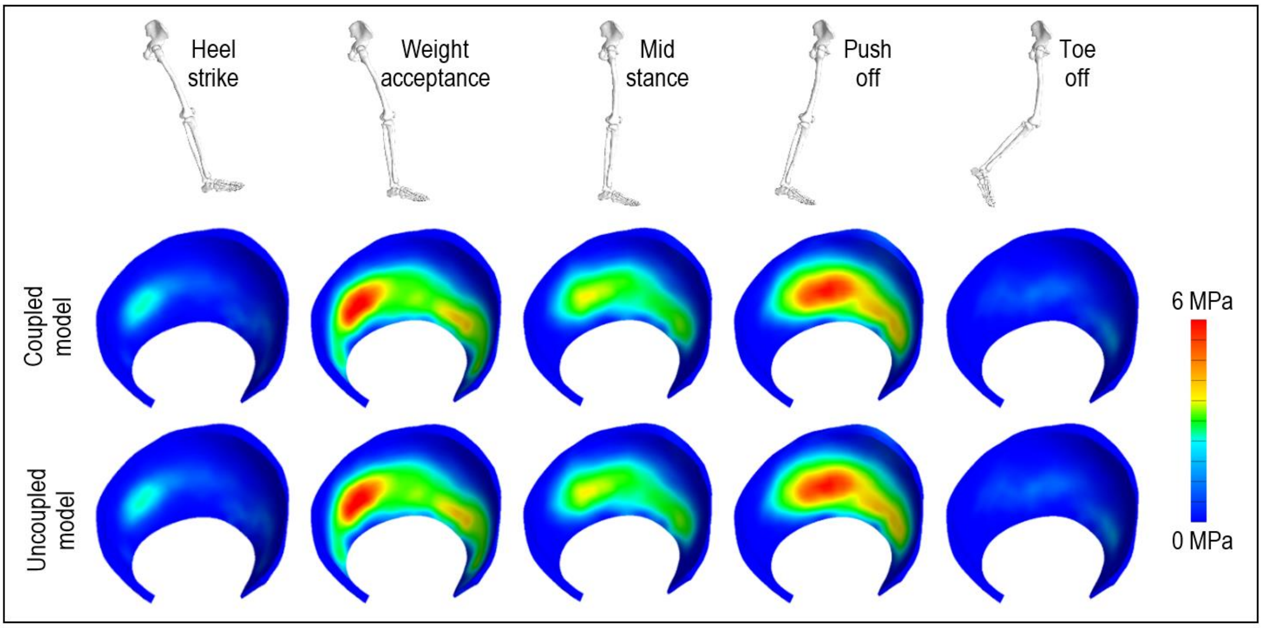
Heel strike
Weight acceptance
Mid stance
Push off
Toe off
Coupled model
Uncoupled model
6 MPa
0 MPa

Fig. 4

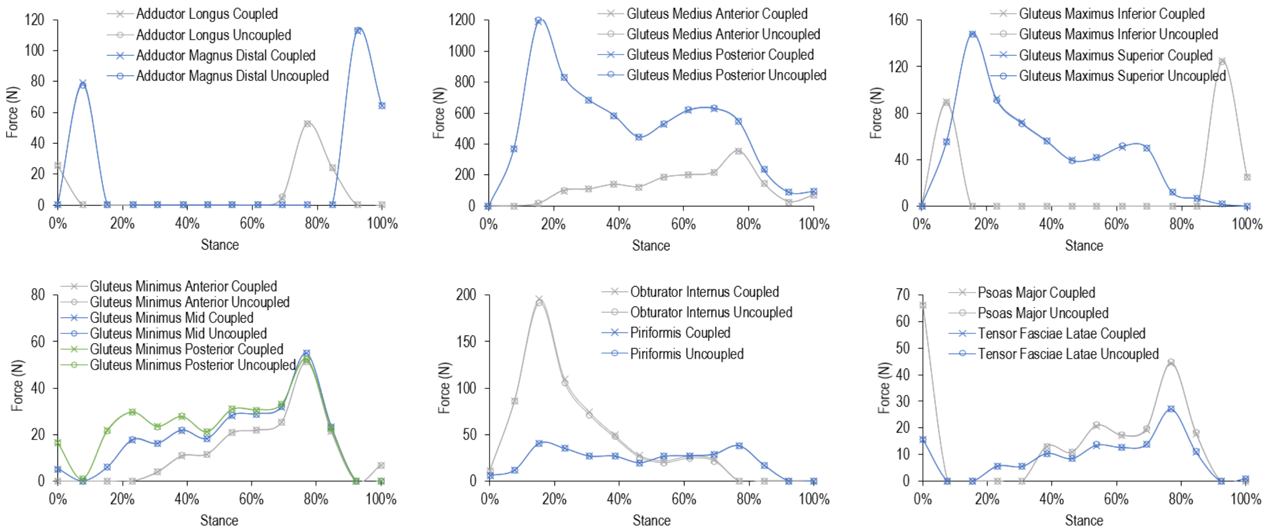

Adductor Longus Coupled
Adductor Longus Uncoupled
Adductor Magnus Distal Coupled
Adductor Magnus Distal Uncoupled
Gluteus Medius Anterior Coupled
Gluteus Medius Anterior Uncoupled
Gluteus Medius Posterior Coupled
Gluteus Medius Posterior Uncoupled
Gluteus Maximus Inferior Coupled
Gluteus Maximus Inferior Uncoupled
Gluteus Maximus Superior Coupled
Gluteus Maximus Superior Uncoupled
Gluteus Minimus Anterior Coupled
Gluteus Minimus Anterior Uncoupled
Gluteus Minimus Mid Coupled
Gluteus Minimus Mid Uncoupled
Gluteus Minimus Posterior Coupled
Gluteus Minimus Posterior Uncoupled
Obturator Internus Coupled
Obturator Internus Uncoupled
Piriformis Coupled
Piriformis Uncoupled
Psoas Major Coupled
Psoas Major Uncoupled
Tensor Fasciae Latae Coupled
Tensor Fasciae Latae Uncoupled
Force (N)
Stance
0% 20% 40% 60% 80% 100%

Fig. 5

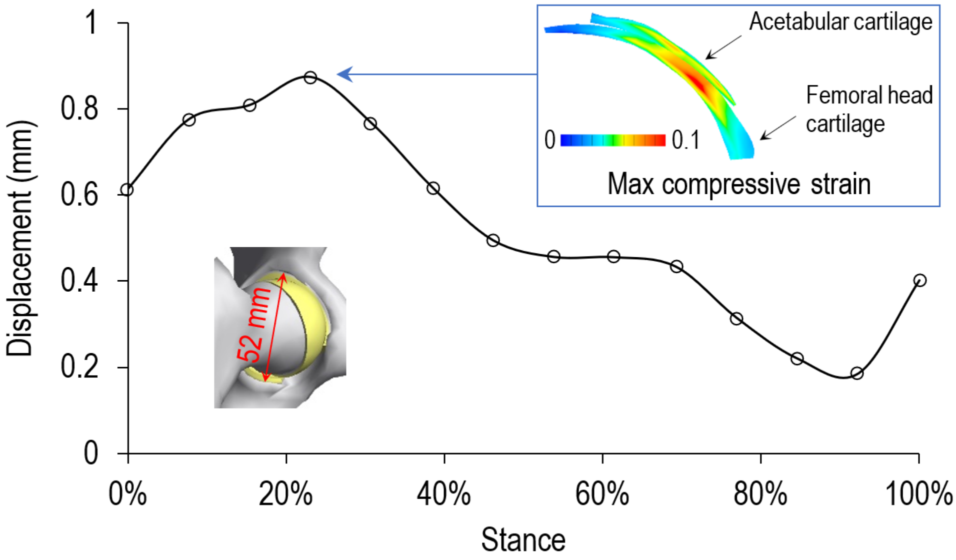

1
0.8
0.6
0.4
0.2
0
Displacement (mm)
0%
20%
40%
60%
80%
100%
Stance
52 mm
Acetabular cartilage
Femoral head cartilage
0
0.1
Max compressive strain